

The Surface Processes on Ru/Pt(111) as Probed by Cyclic Voltammetry and in Situ Surface-Enhanced Raman Spectroscopy

Anni Yu, Rubén Rizo, Francisco J. Vidal-Iglesias, Rosa M. Arán-Ais, Yan-Xia Chen,* Enrique Herrero,* and Juan M. Feliu*



Cite This: <https://doi.org/10.1021/acssuschemeng.2c04584>



Read Online

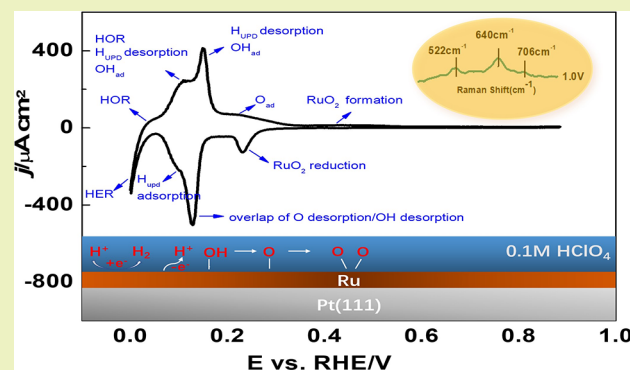
ACCESS |

Metrics & More

Article Recommendations

Supporting Information

ABSTRACT: Information about the chemical adsorption and surface oxidation of Ru under electrochemical conditions is of great importance for understanding the structure–activity relationship in Ru-based materials. Quasi-single-crystalline Ru films on single-crystal Pt(111) electrodes (Ru/Pt(111)) were prepared by the forced-deposition method along with inductive heating treatment. The adsorption of both hydrogen and oxygen species on Ru/Pt(111) was studied by cyclic voltammetry and CO displacement. The potential of zero total charge on Ru/Pt(111) is ca. 0.12 V. A detailed study on oxygen species was carried out by in situ surface-enhanced Raman spectrometry. Ru–O was found to form at $E > 0.1$ V, and the conversion of Ru–O into RuO₂ occurred at $E = 0.3$ V. The reversible oxidation occurs up to 1.0 V. Our results suggest that Ru/Pt(111), which exhibits electrochemical properties similar to those of Ru(0001), may serve as an alternative for Ru study as well as a model system for understanding ligand and strain effects.



KEYWORDS: Electrocatalysis, H adsorption, Surface oxidation, Ruthenium, Cyclic voltammetry, SERS

INTRODUCTION

Ruthenium (Ru) is considered one of the most important metals to be used in the electrocatalysis of many electrochemical energy conversions and storage reactions. Modifying Pt surfaces by Ru atoms is a promising approach to increase the ratio of activity/cost of Pt catalysts toward electrochemical reactions of interest such as the hydrogen evolution/oxidation reaction (HER/HOR)¹ or the methanol oxidation reaction (MOR).² According to the so-called bifunctional mechanism, this improvement can be related to the high oxophilicity of Ru and its ability to provide oxygenated species (OH_{ad} likely) at lower overpotentials than Pt. This bifunctional effect reduces the overpotential for HER/HOR by promoting the Volmer step ($H_2O + e^- \rightarrow *H + OH^-$) as well as the MOR by favoring the oxidation of poisoning intermediates (CO/CH_x) at potential values more negative than Pt. Moreover, Ru itself and Ru-based catalysts have shown promising activity toward the oxygen evolution reaction (OER) due to their moderate capacity to bind oxygen.³

Extensive studies on Ru have shown that its chemical state can greatly affect the adsorption of reaction intermediates and thus its catalytic activity. For example, the HOR was found to be strongly inhibited by the presence of Ru oxides on well-ordered Ru surfaces.⁴ In fact, metallic Ru showed a higher activity for OER than an electrochemically oxidized Ru sample, and this one had higher activity than thermally produced rutile

RuO₂. However, the observed dissolution rate is in an inverse relationship with the OER activity, which reduces its application on OER.^{5,6}

Besides the chemical state, the electroactivity of Ru and Ru-based catalysts can be strongly influenced by the surface structure of Ru. In this sense, the use of well-defined single-crystal electrodes is a powerful approach to systematically studying the structure–activity relationship. Since 1980, the “Clavilier method” of electrode annealing and cooling in an argon/hydrogen atmosphere has enabled the preparation of noble metal single-crystal electrodes, including Pt,⁷ Rh,⁸ Pd,⁹ Au, and Ir¹⁰ without the need for UHV devices. However, this protocol does not work for Ru because it is rapidly oxidized by atmospheric oxygen even at high temperatures. Since the 2000s, several methods were reported to prepare Ru single crystal electrodes under non-UHV conditions, such as the heating of the electrode in a H₂ atmosphere at 1200 °C¹¹ or the mechanical polishing of the electrode combined with electrochemical reduction at very negative potentials.¹²

Received: August 1, 2022

Revised: October 17, 2022

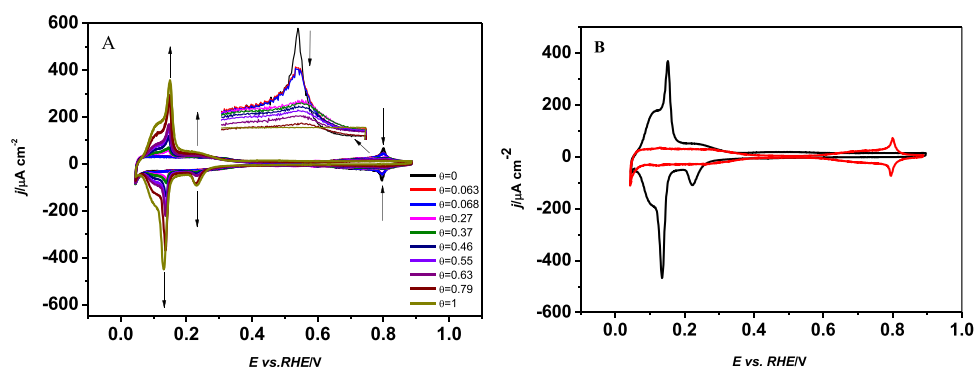


Figure 1. CV curves for Pt(111) and Ru deposited surfaces with (A) different Ru coverages and (B) the maximum Ru coverage (Ru/Pt(111)) in 0.1 M HClO₄ at 50 mV/s.

However, both are time-consuming approaches, and the final surface is rough and heterogeneous after the polishing process. Instead, Kibler et al. presented a method involving inductive heating in an argon atmosphere, which gives a rather clean and well-ordered Ru(0001) surface.¹³ On the other hand, Attard et al. proposed a “forced deposition” method followed by resistive heating in nitrogen to prepare quasi-single-crystalline Ru films on a well-defined Pt single crystal (denoted as Ru/Pt(*hkl*)).¹⁴ The advantage of this method is that the well-established preparation methods for Pt single-crystal electrodes enable the systematic control of the structural properties of the deposited Ru film. Furthermore, because (1) the electronic structure of Ru can be modified by neighboring Pt atoms and (2) there is a lattice mismatch between Ru, which crystallizes in a hexagonal close-packed structure, and Pt, which crystallizes in a face-centered cubic stacking structure, Ru/Pt(*hkl*) can also serve as a model system for understanding the ligand effect and strain effects. In the case of a Pt/Ru alloy formation, both effects might be present. However, for a Ru multilayer system, the ligand effect is not expected to exert any influence when the epitaxial layer is thicker than one monolayer, whereas a strain effect can be expected even if the epitaxial layer is several monolayers thick. Further modification with other elements, such as Pt, will also make it a novel model system for the oxidation of small organic molecules, typically CO and methanol. However, detailed and systematic studies on the surface adsorption processes taking place in this system under electrochemical conditions in aqueous electrolytes are still lacking. In this Article, Ru/Pt(111) surfaces have been prepared via depositing Ru on Pt(111) followed by inductive heating. Electrochemical measurements together with Raman spectroscopy have been used to establish the correspondence between the voltammetric behavior and the electrode surface processes, that is, H adsorption/evolution/oxidation, a possible perchlorate reduction, and the surface oxidation in perchloric acid electrolyte.

EXPERIMENTAL METHODS

Preparation of the Ru/Pt(111) Surfaces. The ruthenium-deposited Pt(111) surfaces were prepared via the forced-deposition method along with inductive heating treatment modified from ref 14. In brief, a Pt(111) single-crystal surface used as a substrate was flame annealed and cooled in an H₂+Ar (1:3) atmosphere. The surface then was characterized by cyclic voltammetry (CV) to confirm the surface order and the electrolyte cleanliness. A 0.01 M RuNO(NO₃)₂ depositing solution was prepared in a small beaker. For the deposition of the Ru film, the characterized Pt(111) substrate was immersed in the RuNO(NO₃)₂ solution nine times and transferred to a H₂ bubbler

for about 5 s. The electrode then was heated in an inductive oven for 50 s in an Ar atmosphere at approximately 1000 K. After being cooled back to room temperature, the electrode was transferred to the electrochemical cell under the protection of a drop of ultrapure water for the voltammetric measurements. By changing the concentration of the Ru depositing solution and the deposition cycles, we could obtain surfaces with different Ru coverages (Figure 1A).

Electrochemical Measurements. The experiments were carried out in a conventional three-electrode cell connected to a signal generator EG&G PARC and eDAQ EA161 potentiostat with an eDAQ e-corder ED401 recording system. A platinum wire was used as a counter electrode, and a reversible hydrogen electrode (RHE) was used as the reference electrode. The electrolyte solutions were prepared using 18.2 MΩ cm Milli-Q water and high-purity chemicals: HClO₄ (Merck p.a.) and CO, Ar, and H₂ (Air products N.V.). Solutions were deaerated with Ar before any electrochemical experiment.

CO Displacement Measurements. The CO displacement method is described elsewhere.¹⁵ In summary, an initial voltammogram is recorded to check the state of the surface and the cleanliness of the electrolyte. The electrode potential then is fixed at the desired value, and CO is introduced into the electrochemical cell. The current response is recorded versus time until a close to zero constant current is obtained. At this point, the CO flux is stopped and Ar is bubbled during the required time to remove all of the CO from the solution. Finally, CO adsorbed on the surface is stripped out by recording a CV up to 0.9 V.

In Situ FTIR Spectrum. In situ Fourier transform infrared (FTIR) spectroscopic measurements were performed with a Nicolet Magna 850 spectrometer equipped with an MCT (mercury–cadmium–telluride) detector. The spectroelectrochemical cell was provided with a prismatic CaF₂ window beveled at 60°. The CO submonolayer was deposited under potentiostatic conditions by using a low gas flow in the electrochemical cell atmosphere. The different spectra (obtained from the average of 100 interferograms with a resolution of 8 cm⁻¹) were collected at potential steps from 0.1 to 0.9 V vs RHE. Spectra are presented in absorbance units ($A = -\log(R/R^0)$), in which *R* and *R*⁰ refer to the reflectance spectra at the sampling and reference potential (0.90 V), respectively.¹⁶ At 0.9 V, CO has been stripped from the surface. All of the spectroelectrochemical experiments were also performed at room temperature in 0.1 M HClO₄ with a reversible hydrogen electrode (RHE) and a gold wire used as the reference and counter electrodes, respectively.

Raman Spectrum. Raman spectra were recorded with an NRS-5100 (Jasco) Raman spectrometer integrated with a confocal microscope. The spectra were obtained by excitation with a 17 mW He–Ne laser with a wavelength of 632.8 nm. Raman was calibrated versus the 520 cm⁻¹ peak of Si with a resolution of 1.0 cm⁻¹. For the Raman enhancement tests, 2.5 μL of Au nanoparticles (~50 nm) were deposited onto the electrode surface by drop casting.

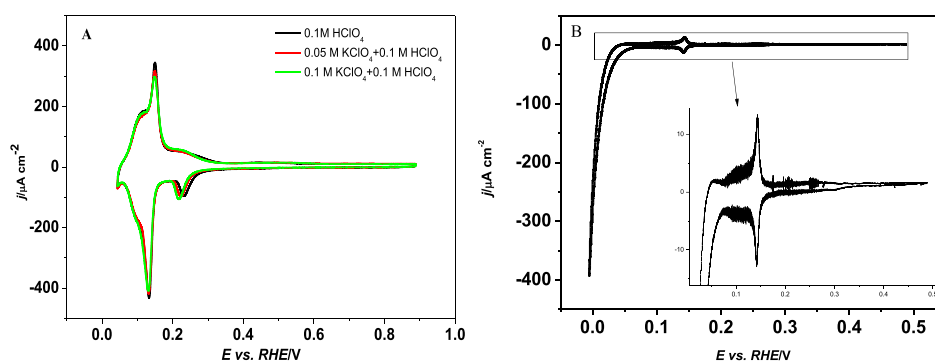


Figure 2. (A) CVs for Ru/Pt(111) in solutions with different perchlorate concentrations at 50 mV/s; and (B) CV for Ru/Pt(111) in 0.1 M HClO₄ at 1 mV/s.

RESULTS AND DISCUSSION

Figure 1 displays the CVs for Pt(111) substrate and the deposited surfaces with different Ru coverages in 0.1 M HClO₄. To distinguish, Ru/Pt(111) is used specifically for a fully covered Ru surface, which is also our main topic. The Pt(111) shows the typical hydrogen adsorption/desorption charge in the range between 0.07 and 0.35 V separated from the OH adsorption/desorption region between 0.55 and 0.90 V by the so-called double layer, in agreement with previous studies.¹⁵ After the modification of the Pt(111) surface with Ru, a gradual decrease in the OH adsorption/desorption region with a simultaneous increase in the currents recorded in the hydrogen adsorption/desorption region of the Pt(111) are observed as the deposition cycles increase from 1 to 9. At this point, the peak at 0.8 V, corresponding to the adsorption of OH on the Pt surface, has completely disappeared. Further increase in the deposition cycles from 9 to 20 (Figure S1) does not result in a change in the voltammetric profiles, indicating that the surface has been completely covered by Ru, reaching the maximum coverage. The absence of a Pt–OH adsorption/desorption charge for the Ru/Pt(111) surface above 0.55 V suggests that the Pt(111) surface is fully covered by Ru.

To determine the presence of different atoms (Pt or Ru) on the surface, in situ FTIR spectra of adsorbed CO on the Pt(111) and the Ru/Pt(111) with maximum Ru coverage surfaces were taken (Figure S2). CO can be used as a probe molecule because the position of the bands depends on the nature of the substrate. Clearly, both sets of spectra are completely different. Moreover, the spectra for the Ru/Pt(111) electrode show no signals for CO adsorption on Pt, which indicates that Pt ensembles are not present on the surface of the Ru/Pt(111) electrode; that is, the Pt(111) surface is fully covered by Ru, and, if Pt atoms are present on the surface, they are probably isolated completely surrounded by Ru atoms. On the basis of the observations above, the coverage of Ru can be calculated using the oxygen adsorption charge according to the following equation:

$$\theta_{\text{Ru}} = (Q_{\text{Pt}}^{\text{O}} - Q_{\text{Pt,Ru}}^{\text{O}}) / Q_{\text{Pt}}^{\text{O}} \quad (1)$$

Q_{Pt}^{O} and $Q_{\text{Pt,Ru}}^{\text{O}}$ are the integral charges of the oxygen adsorption region on clean Pt(111) and the surface after deposition of Ru, respectively.

The Ru/Pt(111) surface in Figure 1B exhibits an asymmetric adsorption/desorption process in the region between 0.05 and 0.35 V with a peak current centered at 0.15 V in the positive scan direction and 0.13 V in the negative scan direction, similar to those previously reported on

Ru(0001).¹⁷ The nature of this contribution will be studied throughout this work. In the positive scan direction, a broad flat peak appears from ca. 0.35 to 0.6 V. Moreover, between 0.6 and 0.90 V, in contrast to Pt(111), the Ru/Pt(111) profile only shows capacitive currents, and no adsorption/desorption process seems to take place over this region.

A similar profile has already been found by Hoster et al. for an UHV-prepared Pt_xRu_{1-x}/Ru(0001) alloy with a low Pt:Ru ratio ($x_{\text{Pt}} < 0.25$), whereas the Ru(0001) surface shows different voltammetric behavior.¹⁸ Thus, it is proposed that Ru deposition followed by annealing in an Ar atmosphere allows the formation of a Pt–Ru(0001) alloy whose morphology is controlled by the morphology of the Pt substrate. It should be stressed that the modification of a polycrystalline Pt with the same method does not lead to the same voltammetric profile, which highlights the role of the surface structure of the substrate in the morphology of the film (Figure S3).

It has been previously shown that, without inductive heating, both spontaneously and electrodeposited ruthenium deposition processes on well-defined Pt(111) electrodes result in the formation of two-dimensional, monatomic islands of ca. 0.5–1 and 2–5 nm in diameter, as revealed by the scanning tunneling microscopy (STM) data.^{19,20} It is worth noting that the deposited Ru layer could be completely removed by flame annealing in a propane/butane flame, as the recovery of the voltammetric profile for the Pt substrate indicates. Additionally, if the voltammetric profiles for the deposited surface after inductive heating suffer changes due to long-time scanning or electrocatalytic reactions, they could be fully recovered by using the same inductive heating conditions as described in the Experimental Methods, which implies that an ordered adlayer of Ru atoms can be formed on the surface by this thermal treatment.

Regarding the interpretation of the voltammograms, the chemical nature of the different processes involved under the different peaks in the CV at potentials below 0.4 V for the Ru/Pt(111) surface is still not well-known. In this sense, the contribution of the perchlorate species (ClO₄⁻) in the peaks from the CV is one of the possible alternatives that has to be explored. It is generally accepted that these species do not adsorb specifically on the Pt surface, although Attard et al. reported the specific adsorption of perchlorate on Pt single-crystal electrodes, from which they concluded in their observation that the cyclic voltammetry is slightly dependent on the perchloric acid concentration.²¹ However, Yi-Fan et al. proposed that the perchlorate anions interact with the OH adlayer, instead of specifically adsorbing onto the Pt(111)

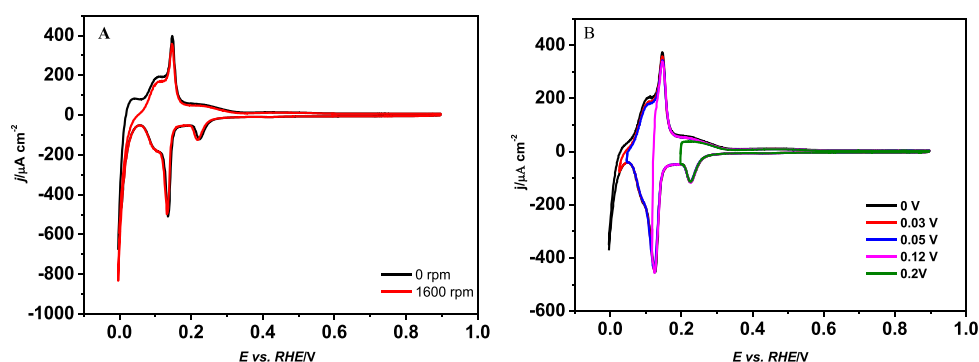
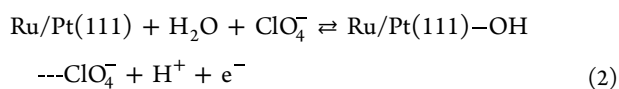


Figure 3. (A) Comparison of the CVs for Ru/Pt(111) under rotational and stationary conditions in 0.1 M HClO₄; and (B) CVs under different lower potential limits in 0.1 M HClO₄. Sweep rate: 50 mV/s.

surface.²² Indeed, no perturbations in the hydrogen adsorption/desorption region were found by Attard et al. by increasing the concentration of perchlorate. Yet, some studies about the electrodeposition of Ru on Pt demonstrated that Ru can reduce perchlorate, although at a very low rate, and it is only detected at low scan rates.²³ To study the interaction of perchlorate with the surface, different perchlorate concentrations were employed while maintaining the pH (Figure 2). As can be observed, the increase in the concentration of perchlorate does not modify the CV for the Ru/Pt(111) surface except for the cathodic peak at ca. 0.23 V, which shifts slightly to negative potentials by increasing the perchlorate concentration. Because the increase in the perchlorate concentration has been studied while maintaining constant the concentration of the H⁺ species in solution, this shift cannot be assigned to a change in the pH but to a different factor. The reduction of the perchlorate interacting specifically with the electrode surface at 0.23 V can also be discarded as the cause of this shift because the same peak was obtained by using a 0.5 M H₂SO₄ solution in the absence of perchlorate anions (Figure S4). Furthermore, higher currents for the cathodic peak at 0.23 V would have been expected at low scan rates (1 mV/s, Figure 2B) if the slow reduction of perchlorate anions had been involved in this peak. However, no changes in the CV with the scan rate were detected. Thus, at this point, we consider that the shift of the cathodic peak at 0.23 V with the perchlorate concentration is related either to the change in the water structure induced by the presence of K⁺ cations or to the perchlorate interaction with adsorbed OH on the surface as follows:



Thus, it is confirmed that the process below 0.4 V in the CV is not dependent on the perchlorate anions and no specific adsorption of such species is observed on the Ru/Pt(111) surface.

However, the nature of the peaks at this potential range (0.05–0.4 V) is still an unsolved question. To help fulfill this query, the CVs from the Ru/Pt(111) surface with and without rotation regime have been compared (Figure 3). During the rotation, hydrogen formed during the negative scan direction due to the hydrogen evolution reaction (HER) is removed from the electrode surface, and thus its oxidation process (the hydrogen oxidation reaction, HOR) is not observed during the positive scan direction. In this way, it is possible to discern

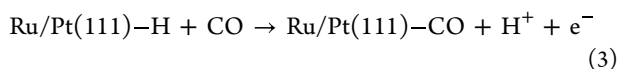
between H₂ production/oxidation and surface redox processes such as H_{ads}/OH_{ads} under the peaks in the region between 0.05 and 0.40 V. As can be observed in Figure 3A, at potentials lower than 0.05 V, the cathodic current increases exponentially, which is attributed to the HER. At around 0 V, the HER is controlled by kinetics so that the current is independent of the electrode rotating rate. As the lower limit potential gradually increases from 0 to 0.05 V (Figure 3B), the current for the HER decreases. Thus, 0.05 V appears to be the onset potential for bulk HER, as confirmed. Our further rotation experiments at different lower limit potentials have confirmed this (Figure S5).

In the positive sweep, the peaks remain unaltered under rotation when compared to the stationary curve except for the small decrease in charge in the shoulders centered at ca. 0.05 and 0.10 V, which might be associated with the oxidation of hydrogen formed during the negative-going scan at potentials close to 0 V. Thus, it discards any possible contribution of the HOR in the main peaks between 0.1 and 0.40 V. Furthermore, CVs recorded in different potential limits (Figure 3b) suggest that the process taking place under the cathodic peak at 0.23 V is independent of the processes occurring under the main peaks located at 0.14 V.

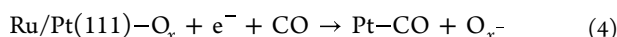
Nevertheless, it is surprising that H₂ formation occurred at potentials more positive than the equilibrium potential of the redox couple H⁺/H₂ (0 V vs RHE). Similar phenomena have also been recently reported on Ru(0001) and polycrystalline Cu.^{24,25} Using electrochemistry-online mass spectrometry, Engstfeld²⁵ and Scott²⁴ observed an H₂ signal at potentials around 0.1 V on Ru(0001), which was denoted as “anodic H₂” to distinguish from the expected H₂ signal from bulk HER at $E < 0$ V. It is suggested that at least part of the hydrogen adsorbed via a Volmer step ($* + \text{H}^+ + \text{e}^- \rightleftharpoons * \text{H}$) at sufficiently negative potentials (HER region) desorbed to form H₂ in the subsequent positive scan direction at potentials > 0 V via a Tafel step ($* \text{H} + * \text{H} \rightleftharpoons \text{H}_2 + 2*$) or Heyrovsky step ($* \text{H} + \text{H}^+ + \text{e}^- \rightleftharpoons \text{H}_2 + *$) instead of the commonly expected H⁺ formation via the reverse Volmer step. The Tafel mechanism was considered more plausible according to a detailed charge evaluation. The key point for this mechanism is that the more favorable OH adsorption at anodic potentials upshifts the free energy of adsorbed H ($G(\text{H}_{\text{ad}})$) making H_{ad} desorption easier while giving a high enough barrier for the Volmer step. An early CO displacement experiment on Ru(0001) in 0.01 M HClO₄ has proved that about 0.4 monolayers (ML) of OH are adsorbed at ca. 0.1 V vs RHE.¹³ To check whether OH is coadsorbed with H at low potentials on Ru/Pt(111) and to

explore the chemical nature under the different peaks, CO displacement measurements were also performed.

As described in the [Experimental Methods](#), CO displacement experiments are performed by CO dosing in the electrochemical cell at a constant potential. CO molecules adsorb on the surface and displace the species previously adsorbed on the Ru/Pt(111) electrode surface. The sign of the registered current transient indicates the charge of the species that have been displaced by CO. In this sense, when the current transients at a certain potential are positive, the total surface charge before the introduction of CO is negative, and thus the main process involved is most probably the displacement of adsorbed hydrogen, according to [reaction 3](#):



Adsorbed oxygenated species on the Ru/Pt(111) surface are responsible for the negative current during the CO displacement, according to [reaction 4](#), because perchlorate has been found previously to not be adsorbed on the electrode surface:



In addition, by calculating the charge displaced by the integration of current transient recorded at potentials where CO is not oxidized, we determined it was possible to build the curve q versus E . According to [eq 5](#), this curve must be the same as the curve obtained by integrating the voltammetric current when the processes occurring are reversible enough to be considered at equilibrium at the recording scan rate:

$$q(E) = \int_{E^*}^E \frac{j}{\nu} dE + q(E^*) \quad (5)$$

where j is the voltammetric current density, ν is the scan rate, and $q(E^*)$ is the integration constant. On the Ru/Pt(111) electrode, CO displacement experiments have been performed at different potential values in the range between 0.09 and 0.23 V. [Figure 4](#) (black line) shows the total charge curve as a

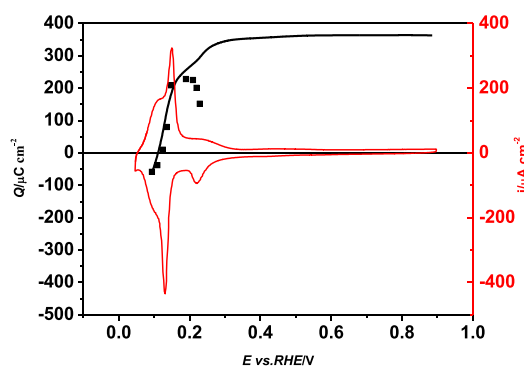
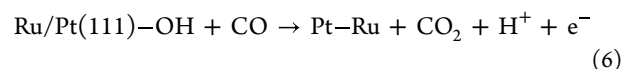


Figure 4. Cyclic voltammogram (red line) and total charge curve (black line) for the Ru/Pt(111) surface as a function of the potential recorded at 50 mV s^{-1} and CO displaced charge at different potentials (■) in 0.1 M HClO_4 solution.

function of the potential, which has been obtained by the integration of the CV employing the value of the charge displaced at 0.09 V as the integration constant ($q(E^*)$ in [eq 5](#)). As expected, the values of the charge displaced by CO overlap with the integrated curve in the range between 0.09 and 0.15 V , which is the region for the main peak in the CV. However, for potentials more positive than 0.17 V , a deviation between

the charge displaced and the integrated curve is observed. In the region between 0.09 and 0.15 V , under the shoulder centered at 0.10 V , the current transient curves in [Figure 5](#) show positive currents up to 0.11 V . Thus, the shoulder before the main peak should be assigned to H_{ads} on the Ru/Pt(111) surface ([reaction 3](#)). However, the CO displacement transients at potentials between 0.11 and 0.13 V reverse the sign and become negative, indicating that oxygenated species are adsorbed on the surface under the main peak as described in [reaction 4](#). The potential of zero total charge on the Ru/Pt(111) surface lies around 0.12 V where the hydrogen and anion (probably OH) adsorption processes contribute in equal amounts but with opposite signs to the total charge. The integrated charge from 0.09 to 0.12 V is only $116.4 \mu\text{C}/\text{cm}^2$, much lower than the charge expected for a one-electron process on Ru ($257 \mu\text{C}/\text{cm}^2$), whereas the integrated voltammetric charge from 0.12 to 0.2 V is $283.3 \mu\text{C}/\text{cm}^2$, very close to the charge for a one-electron transfer process ($257 \mu\text{C}/\text{cm}^2$). Thus, at 0.09 V , hydrogen is adsorbed on the surface with a coverage of ca. 0.5 ML , whereas, at 0.2 V , a full monolayer of adsorbed OH is present on the surface.

Additionally, a deviation of the CO displaced charge values from the integrated curve at potentials more positive than 0.2 V is observed. This deviation can be explained by considering two possible reasons. The first one is that the CO oxidation takes place at 0.17 V as follows:



However, this explanation can be excluded because the CO stripping curves do not show any oxidation current until 0.45 V ([Figure S6](#)). Also, the currents for the transients at long times are zero. The most likely explanation is that oxygen-containing species undergo some transformation, such as further oxidation to high-valent O that cannot be replaced by CO. A detailed ECQM study on the surface oxidation of electrodeposited Ru has supported this idea.²⁶

Surface ruthenium can present several oxide states depending on the potential. Although the Pourbaix diagram of Ru²⁶ shows that Ru exists as a metal up to 0.6 V vs SHE at pH 0–3, numerous studies have reported the Ru surface oxidation to Ru–O at about 0.2 V vs RHE2,^{26,27} in agreement with our CO displacement results (the displacement charge had decreased since 0.2 V). Concerning the formation of the oxide, several reports indicate the formation of Ru surface oxides at low potentials. Szabd and Bakos stated that the valence states of the Ru coatings deposited between 0 and 0.2 V are almost identical,²⁸ which corresponds to RuOH in our case. In situ structural characterization by surface X-ray diffraction (SXRD) on Ru(0001) showed that the decrease in $(0,1-1,1.6)$ intensity from 0.2 to 0.4 V was caused by the change in the topmost Ru interlayer spacing and buckling, indicating the oxidation of $*\text{OH}$ to $*\text{O}$.²⁵ By using EQCM, Sugawara et al. observed a mass loss between 0.2 and 0.5 V and ascribed it to the loss of H^+ to form RuO.²⁶ At potentials between 0.45 and 0.7 V , the Ru(0001) surface was found mostly covered by $*\text{O}$.²⁵ Increasing the upper potential limit from 0.7 to 0.9 V leads to an increase in the size of the cathodic peak in the negative scan direction at 0.23 V , implying higher valence state oxides formed at more positive potentials than 0.7 V .²⁵ Hadzi-Jordanov et al. found that the reversible oxidation on the Pt–Ru alloy occurs up to a potential of 0.8 V .²⁹ Quiroz et al. assumed that the oxide species formed on an electrodeposited

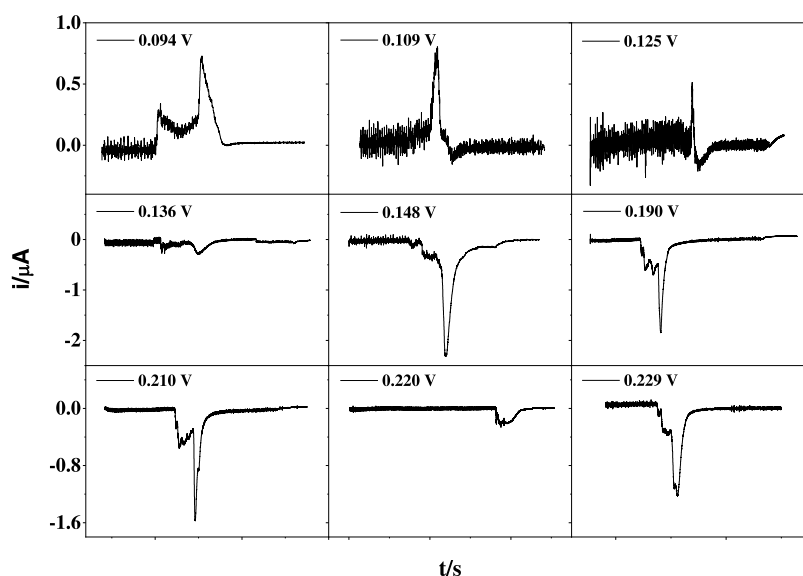


Figure 5. Transient current curves for CO displacement recorded at different potentials in 0.1 M HClO₄ solution.

Ru before 0.8–0.9 V are RuO, and the following oxides are RuO₂,³⁰ and a dissolution study on Ru and ruthenium oxide nanoparticles implied that RuO₂ was stable up to a potential of 1.3 V.⁶

Regarding spectroscopic pieces of evidence on the presence of oxides on the surface, in situ FTIR results were only able to detect the presence of the corrosion oxide RuO₄ at 920 cm⁻¹ in 0.1 M HClO₄.³¹ In this sense, surface-enhanced Raman spectroscopy is a very useful technique due to the sensitivity of SERS to probe metal–oxygen vibrational modes, usually found in the low-frequency region between 200 and 1000 cm⁻¹.^{32–35} The SERS-active Ru film was prepared as described above. The electrode was then transferred rapidly from the electrochemical cell to a SERS cell with aqueous 0.1 M HClO₄ as the supporting electrolyte. Potential-dependent SER spectra of the Ru/Pt(111) film acquired in 0.1 M HClO₄ are shown in Figure 6. The applied potential was initially kept at 0 V for about 5 min in deaerated 0.1 M HClO₄ to reduce the Ru oxide formed during electrode transfer. The typical vibrational spectroscopic data in the literature for several ruthenium oxides are summarized in Table 1 to help in the assignments of the bands we observed in Figure 6.

At 0 V, the Raman spectrum was featureless, indicating the initial surface was clean and unoxidized. The applied potential was then increased progressively up to 1.0 V (vs RHE), holding at each potential for 150 s before the spectra were acquired. For all of the spectra, a band centered at 932 cm⁻¹ appeared, which is assigned to the A₁ mode of Cl–O in perchlorate.^{43–45} The absence of significant changes in the frequency of this band with potential indicates that perchlorate is located near the electrode surface rather than electrochemically adsorbed in the interface, which supports the evidence described below for the experiments using solutions with different concentrations of perchlorate (Figure 2). However, after a close analysis of this band (Figure 6, inset), a small Stark effect^{46,47} can be observed. The latter suggests that this perchlorate is located in the compact part of the interfacial double layer, as proposed by Yi-Fan et al.,²² and that the distance separating both species might be on the order of the length of an OH bond.

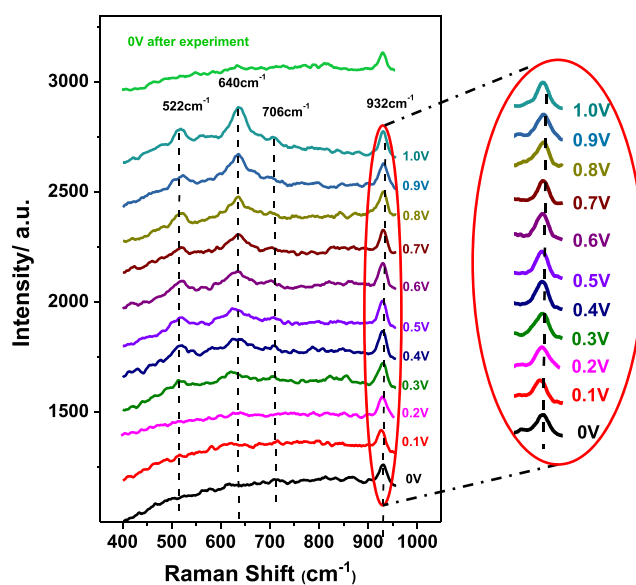


Figure 6. Electrochemical in situ SER spectra obtained for Ru/Pt(111) in 0.1 M HClO₄ as a function of the applied potential (vs RHE). The surface was initially reduced at 0 V (bottom spectrum) before the potential was raised to 1.0 V (where Ru starts to dissolve) and subsequently reduced again at 0 V. The inset shows the magnification of the band at 932 cm⁻¹.

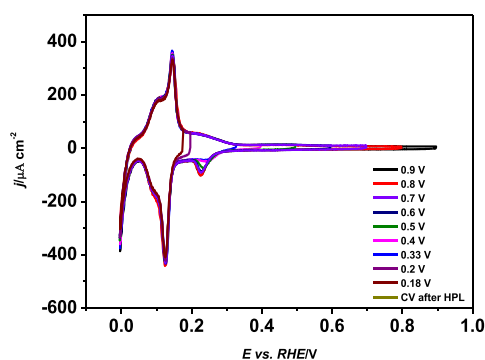
Between 0 and 0.2 V, the spectra were largely featureless. At potentials higher than 0.2 V, a series of bands aroused and grew with the potential in the SER spectra. The 522/640/706 cm⁻¹ pair observed here has frequencies comparable to the characteristic normal Raman bands of anhydrous RuO₂ (Table 1), which are not present for the bare Pt(111) at the same experimental conditions.⁴⁸ Thus, the broad flat signal centered around 0.3 V in the voltammetric profile can be assigned to the formation of RuO₂, and hence it confirms that the deviation between the integrated CV charge and the CO displacement charge in Figure 4 is due to the formation of RuO₂ because the adsorbed O from the oxide cannot be displaced by CO. No additional bands appeared as the potential is gradually increased to 1.0 V. This indicates that higher-valent oxides

Table 1. Published Vibrational Modes of Various Ru Oxides, Oxyanions, and Adsorbed Oxygen on Ru

species	$\nu(\text{Ru}-\text{O})$ stretching modes (cm^{-1})	ref	technique
adsorbed atomic oxygen	250–300/450–500	33	SERS
		34	Raman
	585	36	EELS
	575–595	37	EELS
	520–600	38	EELS
RuO ₂ (hydrous)	470/670	32	SERS
	488	34	Raman
	477	35	Raman
RuO ₂ (anhydrous)	510/630	32	SERS
	515/626	39	Raman
	528/646	40	SERS
	523/646/710	35	Raman
	526/640/715	34	Raman
RuO ₃	800	32	SERS
RuO ₄ ²⁻	808	41	Raman
RuO ₄	875	32	SERS
	878	42	Raman
	881	41	Raman

are not formed within this potential region, which is reasonable because the next oxide state of ruthenium (RuO_4^{2-}) is expected to form at higher potentials, according to the Pourbaix diagram of Ru. The overall oxidation processes during the selected potential region were confirmed to be reversible by the featureless spectra after the surface was reduced again at 0 V.

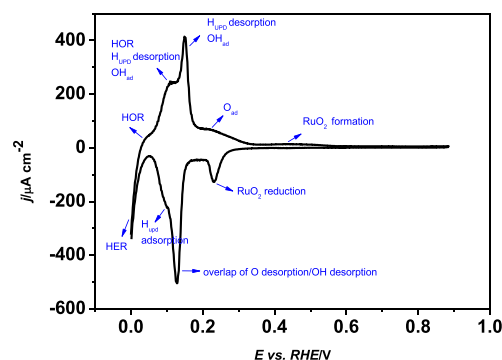
To determine the process related to the small reduction peak around 0.25 V, Figure 7 displayed CVs under different

**Figure 7.** CVs under different upper potential limits in 0.1 M HClO₄ at 50 mV/s.

upper potential limits. The small cathodic peak only appears when the upper potential limit is above 0.33 V, where RuO₂ is detected by SERS. It should be highlighted that 0.33 V corresponds to the upper potential of the broad flat wave observed for the film. So, the reduction peak could apparently be ascribed to the reduction of RuO₂, which formed at high potential. On the basis of the analysis above, the proposed electrochemical surface processes on Ru/Pt(111) in 0.1 M HClO₄ are described in Figure 8.

CONCLUSIONS AND OUTLOOK

In this Article, the quasi-single-crystalline Ru/Pt(111) prepared by the forced-deposition method along with inductive heating treatment was characterized by cyclic

**Figure 8.** Depicted surface processes on Ru/Pt(111) in 0.1 M HClO₄.

voltammetry together with CO displacement and in situ Raman spectrometry. In general, the electrochemical properties of Ru/Pt(111) in perchlorate acid solution were found to be similar to those of Ru(0001). The coadsorption of OH and H at potentials more negative than 0.2 V was confirmed by the observed potential of zero total charge at 0.12 V and charge evaluation. At $E > 0.2$ V, the CO displacement charge decreased due to the formation of Ru–O, as confirmed by the in situ Raman spectrometry experiment. The results obtained from CO displacement and in situ Raman agree well with each other. In addition, the formation of the Ru film in our system is more likely to be a homogeneous atomic layer rather than in islands as was observed in previous literature using spontaneous or electrodeposition. Similar to those single crystals, the surface can also be restored by inductive annealing during experiments. However, so far, we are not able to confirm the formation of a Ru monolayer or multilayer system, but we strongly believe that these results, in combination with the deep characterization of this system at an atomic level (e.g., by STM), can be used as an essential tool for the further investigation of the structure–activity relationship. Anion-specific adsorption, electrocatalytic properties for fuel cell reactions on Ru/Pt(111), and further modification of the Ru/Pt(*hkl*) electrodes also will be presented in future studies.

ASSOCIATED CONTENT

Supporting Information

The Supporting Information is available free of charge at <https://pubs.acs.org/doi/10.1021/acssuschemeng.2c04584>.

Comparison of the CVs for Ru/Pt(111) surfaces prepared after 9 and 20 deposition cycles in the Ru-containing solution, in situ FTIR spectra collected from the (A) Pt(111) and (B) Ru/Pt(111) electrodes during a potential step experiment after the adsorption of CO, CVs for Ru/polycrystalline Pt and Ru/Pt(111) in 0.1 M HClO₄ at 50 mV/s, CVs for Ru/Pt(111) in 0.1 M HClO₄ and 0.1 M H₂SO₄, comparison of the CVs for Ru/Pt(111) under rotational and stationary conditions at different lower limit potentials, and CO stripping on Ru/Pt(111) in 0.1 M HClO₄ (PDF)

AUTHOR INFORMATION

Corresponding Authors

Yan-Xia Chen – Hefei National Research Center for Physical Sciences at Microscale, Department of Chemical Physics, University of Science and Technology of China, Hefei

230026, China; orcid.org/0000-0002-1370-7422;

Email: yachen@ustc.edu.cn

Enrique Herrero – Instituto de Electroquímica, Universidad de Alicante, Alicante E-03080, Spain; orcid.org/0000-0002-4509-9716; Email: herrero@ua.es

Juan M. Feliu – Instituto de Electroquímica, Universidad de Alicante, Alicante E-03080, Spain; orcid.org/0000-0003-4751-3279; Email: juan.feliu@ua.es

Authors

Anni Yu – Hefei National Research Center for Physical Sciences at Microscale, Department of Chemical Physics, University of Science and Technology of China, Hefei 230026, China; Instituto de Electroquímica, Universidad de Alicante, Alicante E-03080, Spain

Rubén Rizo – Instituto de Electroquímica, Universidad de Alicante, Alicante E-03080, Spain; orcid.org/0000-0001-8161-2989

Francisco J. Vidal-Iglesias – Instituto de Electroquímica, Universidad de Alicante, Alicante E-03080, Spain

Rosa M. Arán-Ais – Instituto de Electroquímica, Universidad de Alicante, Alicante E-03080, Spain

Complete contact information is available at:

<https://pubs.acs.org/10.1021/acssuschemeng.2c04584>

Notes

The authors declare no competing financial interest.

ACKNOWLEDGMENTS

We thank Prof. Gary Attard for instructions in the preparation of quasi-Ru films and J. Fernández-Vidal for guidance on the SERS experiments. We gratefully acknowledge the funding by the China Scholarship Council (CSC), the National Natural Science Foundation of China (nos. 22172151 and 21972131), the Ministerio de Ciencia e Innovación (Spain) grant nos. PID2019-105653GB-I00 and FJC2018-038607-I, and Generalitat Valenciana (Spain) grant number PROMETEO/2020/063.

REFERENCES

- (1) Zhu, S.; Qin, X.; Xiao, F.; Yang, S.; Xu, Y.; Tan, Z.; Li, J.; Yan, J.; Chen, Q.; Chen, M. The Role of Ruthenium in Improving the Kinetics of Hydrogen Oxidation and Evolution Reactions of Platinum. *Nat. Catal.* **2021**, *4* (8), 711–718.
- (2) Zhang, Z.; Liu, J.; Wang, J.; Wang, Q.; Wang, Y.; Wang, K.; Wang, Z.; Gu, M.; Tang, Z.; Lim, J. Single-Atom Catalyst for High-Performance Methanol Oxidation. *Nat. Commun.* **2021**, *12* (1), 1–9.
- (3) Li, L.; Wang, P.; Shao, Q.; Huang, X. Recent Progress in Advanced Electrocatalyst Design for Acidic Oxygen Evolution Reaction. *Adv. Mater.* **2021**, *33* (50), 2004243.
- (4) Inoue, H.; Wang, J. X.; Sasaki, K.; Adzic, R. R. Electrocatalysis of H₂ Oxidation on Ru (0001) and Ru (10-10) Single Crystal Surfaces. *J. Electroanal. Chem.* **2003**, *554*, 77–85.
- (5) Cherevko, S.; Geiger, S.; Kasian, O.; Kulyk, N.; Grote, J.-P.; Savan, A.; Shrestha, B. R.; Merzlikin, S.; Breitbach, B.; Ludwig, A. Oxygen and Hydrogen Evolution Reactions on Ru, RuO₂, Ir, and IrO₂ Thin Film Electrodes in Acidic and Alkaline Electrolytes: A Comparative Study on Activity and Stability. *Catal. Today* **2016**, *262*, 170–180.
- (6) Hodník, N.; Jovanović, P.; Pavlišić, A.; Jozinović, B.; Zorko, M.; Bele, M.; Selih, V. S.; Sala, M.; Hočvar, S.; Gaberšček, M. New Insights into Corrosion of Ruthenium and Ruthenium Oxide Nanoparticles in Acidic Media. *J. Phys. Chem. C* **2015**, *119* (18), 10140–10147.

(7) Clavilier, J.; Faure, R.; Guinet, G.; Durand, R. Preparation of Monocrystalline Pt Microelectrodes and Electrochemical Study of the Plane Surfaces Cut in the Direction of the {111} and {110} Planes. *J. Electroanal. Chem. Interfacial Electrochem.* **1980**, *107* (1), 205–209.

(8) Hourani, M.; Wieckowski, A. Electrochemistry of the Ordered Rh (111) Electrode: Surface Preparation and Voltammetry in HClO₄ Electrolyte. *J. Electroanal. Chem. Interfacial Electrochem.* **1987**, *227* (1–2), 259–264.

(9) Cuesta, A.; Kibler, L. A.; Kolb, D. M. A Method to Prepare Single Crystal Electrodes of Reactive Metals: Application to Pd (Hkl). *J. Electroanal. Chem.* **1999**, *466* (2), 165–168.

(10) Motoo, S.; Furuya, N. Hydrogen and Oxygen Adsorption on Ir (111), (100) and (110) Planes. *J. Electroanal. Chem. Interfacial Electrochem.* **1984**, *167* (1–2), 309–315.

(11) Lu, P.-C.; Yang, C.-H.; Yau, S.-L.; Zei, M.-S. In Situ Scanning Tunneling Microscopy of (Bi) Sulfate, Oxygen, and Iodine Adlayers Chemisorbed on a Well-Defined Ru (001) Electrode Prepared in a Non-Ultrahigh-Vacuum Environment. *Langmuir* **2002**, *18* (3), 754–762.

(12) Ou Yang, L.-Y.; Yau, S.-L.; Itaya, K. Scanning Tunneling Microscopy of Sulfur and Benzenethiol Chemisorbed on Ru (0001) in 0.1 M HClO₄. *Langmuir* **2004**, *20* (11), 4596–4603.

(13) El-Aziz, A. M.; Kibler, L. A. New Information about the Electrochemical Behaviour of Ru (0 0 0 1) in Perchloric Acid Solutions. *Electrochem. Commun.* **2002**, *4* (11), 866–870.

(14) Huxter, S. E.; Attard, G. A. A New Method for the Preparation of Ru Quasi Single Crystal Surfaces. *Electrochem. Commun.* **2006**, *8* (11), 1806–1810.

(15) Climent, V.; Feliu, J. M. Surface Electrochemistry with Pt Single-Crystal Electrodes. *Nanopatterned and Nanoparticle-Modified Electrodes* **2017**, 1–57.

(16) Rodes, A.; Rueda, M.; Prieto, F.; Prado, C.; Feliu, J. M.; Aldaz, A. Adenine Adsorption at Single Crystal and Thin-Film Gold Electrodes: An In Situ Infrared Spectroscopy Study. *J. Phys. Chem. C* **2009**, *113* (43), 18784–18794.

(17) Marinkovic, N. S.; Vukmirovic, M. B.; Adzic, R. R. Some Recent Studies in Ruthenium Electrochemistry and Electrocatalysis. *Modern Aspects of Electrochemistry*; Springer: New York, 2008; pp 1–52.

(18) Hoster, H. E.; Janik, M. J.; Neurock, M.; Behm, R. J. Pt Promotion and Spill-over Processes during Deposition and Desorption of Upd-H Ad and OH Ad on PtxRu1-x/Ru (0001) Surface Alloys. *Phys. Chem. Chem. Phys.* **2010**, *12* (35), 10388–10397.

(19) Herrero, E.; Feliu, J. M.; Wieckowski, A. Scanning Tunneling Microscopy Images of Ruthenium Submonolayers Spontaneously Deposited on a Pt (111) Electrode. *Langmuir* **1999**, *15* (15), 4944–4948.

(20) Cramm, S.; Friedrich, K. A.; Geysers, K.-P.; Stimming, U.; Vogel, R. Surface Structural and Chemical Characterization of Pt/Ru Composite Electrodes: A Combined Study by XPS, STM and IR Spectroscopy. *Fresenius. J. Anal. Chem.* **1997**, *358* (1), 189–192.

(21) Attard, G. A.; Brew, A.; Hunter, K.; Sharman, J.; Wright, E. Specific Adsorption of Perchlorate Anions on Pt {hkl} Single Crystal Electrodes. *Phys. Chem. Chem. Phys.* **2014**, *16* (27), 13689–13698.

(22) Huang, Y.-F.; Kooyman, P. J.; Koper, M. T. M. Intermediate Stages of Electrochemical Oxidation of Single-Crystalline Platinum Revealed by in Situ Raman Spectroscopy. *Nat. Commun.* **2016**, *7* (1), 1–7.

(23) Colom, F.; Gonzalez-Tejera, M. J. Reduction of Perchlorate Ion on Ruthenium Electrodes in Aqueous Solutions. *J. Electroanal. Chem. Interfacial Electrochem.* **1985**, *190* (1–2), 243–255.

(24) Scott, S. B.; Engstfeld, A. K.; Jusys, Z.; Hochfilzer, D.; Knosgaard, N.; Trimarco, D. B.; Vesborg, P. C. K.; Behm, R. J.; Chorkendorff, I. Anodic Molecular Hydrogen Formation on Ru and Cu Electrodes. *Catal. Sci. Technol.* **2020**, *10* (20), 6870–6878.

(25) Engstfeld, A. K.; Weizenegger, S.; Pithan, L.; Beyer, P.; Jusys, Z.; Bansmann, J.; Behm, R. J.; Drnec, J. Ru (0001) Surface Electrochemistry in the Presence of Specifically Adsorbing Anions. *Electrochim. Acta* **2021**, *389*, 138350.

- (26) Sugawara, Y.; Yadav, A. P.; Nishikata, A.; Tsuru, T. EQCM Study on Dissolution of Ruthenium in Sulfuric Acid. *J. Electrochem. Soc.* **2008**, *155* (9), B897.
- (27) Kinoshita, K.; Ross, P. N. Oxide Stability and Chemisorption Properties of Supported Ruthenium Electrocatalysts. *J. Electroanal. Chem. Interfacial Electrochem.* **1977**, *78* (2), 313–318.
- (28) Szabó, S.; Bakos, I. Investigation of Ruthenium Deposition onto a Platinized Platinum Electrode in Sulfuric Acid Media. *J. Electroanal. Chem. Interfacial Electrochem.* **1987**, *230* (1–2), 233–240.
- (29) Hadz, S.; Angerstein-Kozłowska, H.; Vuković, M.; Conway, B. E. Reversibility and Growth Behavior of Surface Oxide Films at Ruthenium Electrodes. *J. Electrochem. Soc.* **1978**, *125* (9), 1471.
- (30) Quiroz, M. A.; Meas, Y.; Lamy-Pitara, E.; Barbier, J. Characterization of a Ruthenium Electrode by Underpotential Deposition of Copper. *J. Electroanal. Chem. Interfacial Electrochem.* **1983**, *157* (1), 165–174.
- (31) Bewick, A.; Gutiérrez, C.; Larramona, G. In-Situ IR Spectroscopy Study of the Ruthenium Electrode in Acid and Alkaline Solutions. *J. Electroanal. Chem.* **1992**, *332* (1–2), 155–167.
- (32) Chan, H. Y. H.; Takoudis, C. G.; Weaver, M. J. High-Pressure Oxidation of Ruthenium as Probed by Surface-Enhanced Raman and X-Ray Photoelectron Spectroscopies. *J. Catal.* **1997**, *172* (2), 336–345.
- (33) Zhang, Y.; Gao, X.; Weaver, M. J. Nature of Surface Bonding on Voltammetrically Oxidized Noble Metals in Aqueous Media as Probed by Real-Time Surface-Enhanced Raman Spectroscopy. *J. Phys. Chem.* **1993**, *97* (33), 8656–8663.
- (34) Yang, H.; Yang, Y.; Zou, S. Surface-Enhanced Raman Spectroscopic Evidence of Methanol Oxidation on Ruthenium Electrodes. *J. Phys. Chem. B* **2006**, *110* (35), 17296–17301.
- (35) Bhaskar, S.; Dobal, P. S.; Majumder, S. B.; Katiyar, R. S. X-Ray Photoelectron Spectroscopy and Micro-Raman Analysis of Conductive RuO₂ Thin Films. *J. Appl. Phys.* **2001**, *89* (5), 2987–2992.
- (36) Xie, J.; Mitchell, W. J.; Lyons, K. J.; Wang, Y.; Weinberg, W. H. Observation of the Reaction of Gas-phase Atomic Hydrogen with Ru (001)-p (1×2)-O at 100 K. *J. Vac. Sci. Technol. A Vacuum, Surfaces, Film.* **1994**, *12* (4), 2210–2214.
- (37) Mitchell, W. J.; Xie, J.; Lyons, K. J.; Weinberg, W. H. Dissociative Chemisorption of Oxygen on the Ru (001) Surface: Spectroscopic Identification of Precursor Intermediates at Low Surface Temperatures. *J. Vac. Sci. Technol. A Vacuum, Surfaces, Film.* **1994**, *12* (4), 2250–2254.
- (38) Thomas, G. E.; Weinberg, W. H. High Resolution Electron Energy Loss Spectroscopy of Chemisorbed Carbon Monoxide and Oxygen on the Ruthenium (001) Surface. *J. Chem. Phys.* **1979**, *70* (2), 954–961.
- (39) Mar, S. Y.; Chen, C. S.; Huang, Y. S.; Tiong, K.-K. Characterization of RuO₂ Thin Films by Raman Spectroscopy. *Appl. Surf. Sci.* **1995**, *90* (4), 497–504.
- (40) Huang, Y. S.; Pollak, F. H. Raman Investigation of Rutile RuO₂. *Solid State Commun.* **1982**, *43* (12), 921–924.
- (41) Kötz, R.; Stucki, S.; Scherson, D.; Kolb, D. M. In-Situ Identification of RuO₄ as the Corrosion Product during Oxygen Evolution on Ruthenium in Acid Media. *J. Electroanal. Chem. Interfacial Electrochem.* **1984**, *172* (1–2), 211–219.
- (42) Lee, D. G.; van den Engh, M. The Oxidation of Organic Compounds by Ruthenium Tetroxide. *Organic Chemistry*; Elsevier: New York, 1973; Vol. 5, pp 177–227.
- (43) Hester, R. E.; Plane, R. A.; Walrafen, G. E. Raman Spectra of Aqueous Solutions of Indium Sulfate, Nitrate, and Perchlorate. *J. Chem. Phys.* **1963**, *38* (1), 249–250.
- (44) Ratcliffe, C. I.; Irish, D. E. Vibrational Spectral Studies of Solutions at Elevated Temperatures and Pressures. VI. Raman Studies of Perchloric Acid. *Can. J. Chem.* **1984**, *62* (6), 1134–1144.
- (45) Tian, Z.-Q.; Ren, B. Adsorption and Reaction at Electrochemical Interfaces as Probed by Surface-Enhanced Raman Spectroscopy. *Annu. Rev. Phys. Chem.* **2004**, *55*, 197–229.
- (46) Bishop, D. M. The Vibrational Stark Effect. *J. Chem. Phys.* **1993**, *98* (4), 3179–3184.
- (47) Condon, E. U. Production of Infrared Spectra with Electric Fields. *Phys. Rev.* **1932**, *41* (6), 759.
- (48) Sugimura, F.; Sakai, N.; Nakamura, T.; Nakamura, M.; Ikeda, K.; Sakai, T.; Hoshi, N. In Situ Observation of Pt Oxides on the Low Index Planes of Pt Using Surface Enhanced Raman Spectroscopy. *Phys. Chem. Chem. Phys.* **2017**, *19* (40), 27570–27579.